

DMD #53082

Aldehyde Oxidase 1 in Human Liver Cytosols: Quantitative Characterization of AOX1 Expression Level and Activity Relationship

Cexiong Fu, Li Di, Xiaogang Han, Cathy Soderstrom, Mark Snyder, Matthew D. Troutman, R. Scott Obach, Hui Zhang

Department of Pharmacokinetics, Dynamics, and Metabolism, Pfizer Worldwide Research and Development, Pfizer, Inc., Groton, Connecticut (C. F., X. H., C. S., M.D.T., R.S.O., H.Z.) and Scienion US, Inc., Monmouth Junction, New Jersey (M.S.)

DMD #53082

AOX1 Expression Level and Activity Relationship

Address correspondence to: Dr. Hui Zhang, Department of Pharmacokinetics, Dynamics, and Metabolism, Pfizer Worldwide Research and Development, Pfizer, Inc., Mailstop 8220-2155, Groton, CT 06340. E-mail: hui.zhang3@pfizer.com

Number of text pages:	16
Number of tables:	2 (and 1 more supplemental table)
Number of figures:	6
Number of references:	35
Number of words in abstract:	239
Number of words in introduction:	642
Number of words in discussion:	955

List of nonstandard abbreviations:

- AOX1: aldehyde oxidase 1
- CL *int.*: intrinsic clearance
- ELISA: enzyme linked immunosorbent assay
- HLM: human liver microsome
- LC: liquid chromatography
- MRM: multiple reaction monitoring
- MS: mass spectrometry
- SNP: single nucleotide polymorphism

DMD #53082

Abstract

Aldehyde oxidase 1 (AOX1) is a cytosolic enzyme highly-expressed in liver and plays a key role in metabolizing drugs containing aromatic azaheterocyclic substituents. Rapid metabolism catalyzed by AOX1 can cause a drug to exhibit high clearance, low exposure, and hence decreased efficacy or even increased toxicity (if AOX1 generated metabolites are toxic). There is a need to develop the correlation between AOX1 expression levels and AOX1-substrate clearance. A fast, sensitive and robust absolute quantification LC-MS/MS method was developed to quantify AOX1 in human liver cytosol for the first time. This LC-MS/MS method includes a straightforward ultrafiltration fractionation step and gives great selectivity and wide dynamic range (5.2 pM to 20.7 nM). The AOX1 levels in human liver cytosols of 20 donors were quantified using this method to investigate individual differences in AOX1 expression. No significant individual or gender differences in AOX1 levels were observed, although male exhibited a broader distribution than that of female (0.74 to 2.30 pmol/mg vs. 0.74 to 1.69 pmol/mg). The AOX1 protein levels measured by LC-MS/MS were consistent with those measured by an ELISA assay. Several donors have normal AOX1 protein level, but low enzyme activity, which might be due to cofactor deficiency, single nucleotide polymorphism (SNP) or homodimer dissociation. Cytosols from donors with chronic alcohol consumption had low AOX1-catalyzed carbazeran oxidation activities (< 51 $\mu\text{l}/\text{min}/\text{mg}$ compared to a median value of 455 $\mu\text{l}/\text{min}/\text{mg}$), but preserved similar AOX1 protein expression levels (~15% less than the median value).

DMD #53082

Introduction

Aldehyde oxidase 1 (AOX1), a key xenobiotic-metabolizing enzyme, is a member of molybdo-flavoprotein enzyme family that primarily catalyzes two metabolic pathways: 1) hydroxylation of aromatic N-heterocycles and 2) oxidation of aldehydes to the corresponding carboxylic acids (Pryde et al., 2010; Garattini and Terao, 2011). Aromatic heterocycles are key scaffolds to build pharmacophores in medicinal chemistry and a number of these compounds are putative substrates of AOX1. AOX1 can play an important role in metabolic clearance of drugs containing aromatic azaheterocyclic substituents (e.g. zaleplon, brimonidine). Also, AOX1 bioactivation of prodrugs is exemplified in famciclovir, which is bioactivated to the potent antiviral agent penciclovir, which suffers from low oral bioavailability due to poor solubility (Rashidi et al., 1997). In addition to its drug metabolism function, AOX1 is also involved in regulation of reactive oxygen species homeostasis (Li et al., 2009). Furthermore, abundant amounts of AOX1 has been observed in adipose tissue and is proposed to play a critical role in adipogenesis and lipid metabolism by modulating peroxisome proliferator-activated receptor-alpha (PPAR α) (Neumeier et al., 2006; Weigert et al., 2008). Accurate quantitation of AOX1 levels in liver cytosol will enhance our understanding of the pharmacological and toxicological effects of drugs and new drug candidate as well as our understanding of the role of this enzyme in physiological functions.

Expression levels and prevalent isoforms of Aldehyde Oxidase are drastically different between human and preclinical species, which can be a source of cross-species differences in drug metabolic profiles (Dalvie et al., 2010; Diamond et al., 2010). Currently, human tissue expressions of AOX1 were largely estimated by semi-quantitative techniques such as tissue-specific mRNA PCR assay (Garattini and Terao, 2011) and immunohistochemical staining (Moriwaki et al., 2001). According to these studies, liver and adrenal gland are the primary human tissues expressing high levels of AOX1. LC-MS based quantitation methods have emerged as a promising approach for protein quantitation owing to its selectivity, robustness, high-throughput and capacity of multiplexing. In a typical LC-MS quantitation workflow, a protein of interest is digested into small proteotypic peptides by proteases with high substrate

DMD #53082

specificity (e. g. trypsin, Lys-C). Next, a set of suitable proteotypic peptides from the target protein are selected as surrogate measures of protein concentrations. A multiple reaction monitoring (MRM) acquisition method is employed for peptide quantification in conjunction with LC separation (Anderson and Hunter, 2006). In this method, the targeted peptides are first separated by LC. The resolved peptides in LC eluent are ionized into gas phase, and introduced into mass spectrometer for detection. In the MRM mode, targeted peptide ions are preselected through the first mass filter and fragmented by collisional excitation. Fragment ions are then introduced through a second mass filter with preset masses so that only certain sequence-specific fragment ions can be mass analyzed. Compared with the full scan MS/MS mode, the MRM mode greatly enhances detection selectivity, sensitivity, and duty cycle of targeted peptides. This LC-MS/MS method has enabled the development of a wide array of precise and robust protein quantitation assays for clinical samples (Carr and Anderson, 2008; Fernandez Ocana et al., 2012). There is a great interest in quantifying endogenous human drug metabolizing enzymes and drug transporters to assist better understanding the ADME of drugs. LC-MS/MS based quantitation of CYP450 enzyme family (Seibert et al., 2009; Sakamoto et al., 2011; Williamson et al., 2011; Heikkinen et al., 2012), transporters (Li et al., 2008; Sakamoto et al., 2011), UDP-glucuronosyltransferases (UGT) (Sakamoto et al., 2011) have been reported in the literature to assist the development of predictive clearance models. In this report, we described a fast, sensitive and robust LC-MS/MS method to quantify absolute AOX1 levels and the method was applied to AOX1 quantification of human liver cytosol. Accurate quantitation of AOX1 levels in human liver cytosol will help develop scaling factors for *in vitro* - *in vivo* correlation (IVIVC).

DMD #53082

Materials and Methods

Human liver cytosol samples were purchased from Celsis In Vitro Inc. (Baltimore, MD) including twenty different individual lots (M01-M10: ten male donors and F01-F10: ten female donors, listed in supplemental Table 1) as well as a pooled lot (Mix01, pooled from five male and five female donors). Recombinant human AOX1 was ordered from Origene (Rockville, MD). Rapigest SF was from Waters (Milford, MA). Stable heavy isotope labeled and light standard peptides were obtained from New England Peptide (Gardner, MA). Mass spectrometry grade trypsin was acquired from Promega (Madison, WI). Urea, iodoacetamide, dithiothreitol and other chemicals were from Sigma-Aldrich (St. Louis, MO), unless stated otherwise.

Surrogate Peptide Mapping and Selection

For peptide mapping, an aliquot of 5 μ g of recombinant AOX1 was mixed with 4 volumes of 50 mM ammonium bicarbonate buffer (pH 8.0). AOX1 protein was reduced by 5 mM dithiothreitol at 37°C for 30 min and followed by 10 mM iodoacetamide for 10 min in the dark. The final solution was incubated with 0.2 μ g of trypsin overnight with mild agitation. The tryptic peptide solution was acidified with 10% formic acid and 20 μ l of peptide sample was injected onto a fused-core C-18 column (Kinetex 50x2.1 mm, 2.6 μ m, Phenomenex, Torrance, CA) by a CTC PAL autosampler (Leap Technologies, Carrboro, NC). A 14-minute gradient was delivered by a Shimadzu 20D HPLC system at a flow rate of 350 μ l/min using the following gradient: 0min, 5% B; 10min, 40% B; 10.5-12 min, 80% B; 12.01-14 min, 5% B (Mobile phase A is 0.1% formic acid in water and mobile phase B is 0.1% formic acid in acetonitrile). A Triple TOF 5600 mass spectrometer (AB Sciex, Foster City, CA) was used for data acquisition using information dependent acquisition (IDA) mode. Briefly, a full MS1 scan was performed first and the top 20 peptide-like precursor ions (m/z range 400-2000, +2 to +5 charges) in each MS1 scan were selected and fragmented to generate MS/MS spectra. Each precursor ion was excluded for a span of 20 sec after two acquisitions. Peptide identification was performed on ProteinPilot software (AB Sciex,

DMD #53082

Foster City, CA) using the Paragon algorithm. Peptide mapping results were imported into MRMPilot software (AB Sciex, Foster City, CA) to build MRM transitions in high-resolution mode (targeted MRM^{HR} method).

Aliquots of ~ 1 mg human liver cytosols (50 μ l) were mixed with 150 μ l of 8 M urea with supplement of protease inhibitor cocktail. After brief sonication, protein samples were reduced by 5 mM dithiothreitol at 37°C for 30 min followed by incubation in 10 mM iodoacetamide for 10 min in the dark. Small molecules and low-molecular-weight protein interferences were removed by ultrafiltration with 50 kDa MWCO membrane (Millipore, Billerica, MA) according to the manufacturer's protocol. Retentates were recovered and reconstituted in 0.1% Rapigest and 50 mM ammonium bicarbonate (pH 8.0) digestion buffer and incubated overnight at 37°C with a trypsin/protein ratio of 1 to 50. Dog cytosols were prepared in the same manner and used as matrix solution for standard curve preparation. A cocktail of stable labeled forms of surrogated peptides served as internal standards. The digested cytosolic samples were re-injected and all AOX1 peptides of interest were monitored using the targeted MRM^{HR} method. Three peptides were selected for the final quantitation assay.

LC-pseudoMRM Quantitation on a UPLC-LTQ Velos Platform

Peptide mixtures were separated by a 15-min gradient on a Waters Acquity UPLC system (Milford, MA) at a flow rate of 150 μ l/min. Mobile phase A consisted of 0.1% formic acid in HPLC grade water and mobile phase B contains 0.1 % formic acid in LC-MS grade methanol. The LC gradient was initiated with a ramp of 12%B to 48%B in 9 min and followed by a steep increase to 95%B in 2 min. The column was washed with 95% B for 1 min and re-equilibrated under initial conditions for 3 min. The inlet flow was switched online with the mass spectrometer at 1 min and diverted to waste at 13 minute. A LTQ Velos mass spectrometer (Thermo Scientific, Waltham, MA) was operated in the selected ion mode (SIM) for targeted peptide ions. Typical spray voltage, S-lens voltage, heater temperature, and capillary temperature were set to 3.5 kV, 60%, 200°C, and 250°C, respectively. Precursor ions were fragmented in

DMD #53082

the collision cell filled with helium gas at the following settings: 10 millisecond of activation time, 25% normalized collision energy, and 0.25 Q. Peptide quantitation was carried out by integrating area-under-curve (AUC) of each transition and the whole process was automated in Xcalibur Quan Browser.

***In Vitro* AOX1 Activity Assay Using Human Liver Cytosols**

To evaluate the AOX1 activity in various cytosol samples, three probe substrates (carbazeran, zoniporide, and phthalazine) were incubated with liver cytosol samples separately, using an automated procedure on a Sciclone ALH 3000 workstation (Caliper Life Sciences, Hopkinton, MA). Cytosol samples were freshly thawed before incubation and diluted to 1 mg/ml protein concentration in 100 mM potassium phosphate buffer (pH 7.4). The incubation was initiated with addition of substrate (1 μ M, final organic vehicle concentration was 0.01% dimethyl sulfoxide and 0.6% acetonitrile) in a total reaction volume of 200 μ l. Reactions were quenched by addition of cold acetonitrile containing 0.1 μ M CP-628347 (from Pfizer compound library, as an internal standard) at 0, 0.5, 3, 10, 30, 90, 270 min, respectively. Samples were then centrifuged at 3,000 rpm (GH3.8A rotor; Beckman Coulter, CA) for 15 min at room temperature. A 50- μ l aliquot of supernatant was combined with equal volume of water and ready for LC-MS analysis. All incubations were performed in quadruplicates.

Bioanalytical Methods for AOX1 Activity Assay

Aliquots of 20 μ l of cytosol incubation samples were introduced onto a Synergi hydro-RP (2 \times 10 mm, 2.5 μ m; Phenomenex, Torrance, CA) column with an Aria multiplexing autosampler (Thermo Scientific, Waltham, MA). An integrated HPLC pumping system (Shimadzu Scientific Instruments, Columbia, MD) was used for solvent delivery. Samples were then eluted and detected by an API 4000-Qtrap mass spectrometer (AB Sciex, Foster City, CA) equipped with a Turbo IonSpray source. The mobile phase A consisted of 95:2.5:2.5% (2 mM ammonium acetate: methanol: acetonitrile, v/v/v%) (MPA) and 90:9.9:0.1% acetonitrile:water:formic acid (v/v/v%) (MPB). The LC flow rate was 0.6 ml/min. To shorten analysis time, mobile phase was held at 100% MPA for 10 sec then switched to 100% MPB for 15 sec

DMD #53082

(for elution) before returning to 100% MPA for re-equilibration. A two-column switch design was used for increased throughput; while one column was in-line with the mass spectrometer for data acquisition, the other column was undergoing sample injection or column re-equilibration. Multiple reaction monitoring was used to monitor test compounds. The ionization condition and m/z transitions are listed in Table 1 for the three compounds used in AOX1 depletion assays. Peak area ratio of analyte-to-internal standard was calculated for each injection and used to determine substrate depletion rate. *In vitro* intrinsic clearance values of each cytosol lot were calculated from measured half lives ($T_{1/2}$) using following equation.

$$CL_{\text{int, in vitro}} = \ln 2 \times \frac{1}{T_{1/2}(\text{min})} \times \frac{\text{mL incubation}}{1 \text{ mg cytosol protein}} \times \frac{1000 \mu\text{L}}{1 \text{ mL}} = \mu\text{L}/\text{min}/\text{mg} \quad (\text{Eq. 1})$$

ELISA Methods

A sandwich ELISA method was developed to assess AOX1 protein concentrations in human liver cytosols. Anti-AOX1 antibody (Sigma-Aldrich Corp, St. Louis, MO) was coated on to black Maxisorp plates (Nalge-Nunc, Rochester, NY) by dilution in PBS and overnight incubation at 4°C. Recombinant human AOX-1 protein (OriGene USA, Rockville, MD) was serially diluted in an IP lysis buffer (Pierce Chem, Rockford, IL) as a calibration standard from 5 $\mu\text{g}/\text{mL}$ down to 20 ng/mL . Human liver cytosol samples were serially diluted in the same lysis buffer and tested at several dilutions. Samples were incubated on plates, shaking at room temperature for one hour. Unbound protein was washed away with a PBS wash buffer. Bound protein was detected by incubation with biotinylated anti-AOX1 antibody (Sigma-Aldrich Corp.) for one hour, shaking, at room temperature. The plate was washed again to remove unbound antibody and incubated with HRP-streptavidin (Jackson ImmunoResearch Labs, West Grove, PA) for thirty minutes, shaking at room temperature. The plate was washed and signal was developed by addition of SuperSignal Pico ELISA substrate (Pierce Chem) and detected on a luminometer (Victor3 plate reader, Perkin-Elmer, Waltham, MA). Concentrations of AOX1 protein for each sample were determined by comparison of sample signal output to the rhAOX1 calibration curve,

DMD #53082

fitted to a four-parameter logistic regression. The dynamic range of the assay is roughly 35 ng/mL to 5 µg/mL.

Results

Peptide Mapping of AOX1 Protein and MRM Method Development

To establish a robust LC-MS/MS quantitation method, a peptide mapping experiment was first conducted on tryptic digests of AOX1 protein standard using a high resolution hybrid tandem mass spectrometer. The workflow of peptide mapping and targeted MRM^{HR} on a high resolution TripleTOF 5600 instrument incorporated three preliminary steps: 1) peptide mapping of purified protein and endogenous liver cytosol samples, 2) selection of surrogate peptide candidates, and 3) optimization of MRM transitions without the need of peptide standards in the screening stage. Under optimized digestion condition, 84.5% sequence coverage was achieved for the recombinant AOX1 protein. A total of 291 distinct peptides were assigned as fragments from AOX1 and 165 of them were above 95% confidence level. A similar peptide mapping experiment was performed on a crude liver cytosol digestion without fractionation. In the unfractionated cytosol sample, AOX1 protein sequence coverage decreased to 13.3% and only 9 unique peptides were identified with confidence level above 95% out of 219 distinct peptides detected, indicating significant ion suppressing effect of coelutents in the unfractionated liver cytosol digests. A list of 33 peptides were preselected using MRMPilot software for further evaluation, in which all 33 peptides were monitored in digested cytosol samples using a targeted high resolution MRM (MRM^{HR}) experiments. Several stringent filter criteria were applied to select suitable surrogate peptides for AOX1 protein quantitation as follows: 1) select peptides that are specific to human AOX1; 2) avoid sequences containing known SNPs; 3) peptide length from 7 to 18 amino acids; 4) avoid labile amino acids including methionine, tryptophan and cysteine; 5) avoid peptides susceptible to miscleavage; and 6) select peptides with favorable ionization and fragmentation characteristics. After careful screening, three AOX1 peptides (⁴⁴⁶VFFGEGDGIIR⁴⁵⁶, ⁷⁷⁹YIQDIVASTLK⁷⁸⁹ and ⁸¹³TGIIAAVTAFANK⁸²⁶,

DMD #53082

abbreviations as VFF, YIQ and TGI hereafter) with three transitions each were selected as surrogate measures for AOX1 quantity in human liver cytosols.

Figure 1 (top and middle panels) shows the performance of established MRM transitions of three peptides in different matrices using the targeted MRM^{HR} method. VFF peptide yielded the most intense signal among the three peptides, while TGI peptide attained the lowest signal in all experiments. While minor chromatographic overlapping was observed for VFF and YIQ peptides, the specificity of the MRM transitions excluded potential cross-interferences for peak quantitation (as shown by the absence of interfering peak in both chromatograms). In our case, all three transitions for each peptide co-eluted tightly together and consistent ratios between individual transition profiles also confirmed the purity of peptide peaks. A comparison of AOX1 in blank buffer (Figure 1, upper panel) vs. human liver cytosol (Figure 1, middle panel) showed that the retention time for all three peptide peaks were delayed slightly in liver cytosol. There was a concomitant loss of signal intensity primarily due to matrix interference.

Taking advantage of the highly efficient ion fragmentation and trapping of the LTQ Velos instrument, the targeted MRM^{HR} method were transferred from the TripleTOF 5600 platform to a pseudoMRM method to quantify AOX1 levels in human liver cytosols. Representative chromatograms of the three surrogate AOX1 peptides extracted from liver cytosol were illustrated in Figure 1 (bottom panel). There were good agreements of daughter ion selections for the three most intense transitions across the two platforms. Notably, these samples analyzed by the LTQ Velos were five-fold more diluted than the samples shown in MRM^{HR} by TripleTOF 5600 (middle panel) while the peaks intensities still afforded a 3-fold enhancement on average. For this reason (superior detection sensitivity), LTQ Velos platform was chosen for the final AOX1 quantitation in human liver cytosols.

AOX1 Quantitation in Human Liver Cytosols

Since liver cytosol is a common matrix to study AOX1-catalyzed metabolism, the LC-MS/MS method was applied to quantitate AOX1 levels in human liver cytosol samples. Figure 2 showed the linear

DMD #53082

calibration curve for VFF peptide covering the range from 6.25 pg/ml to 25 ng/ml. The linear regression gave an equation of $Y=1.423X - 0.1313$ and R^2 of 0.9994. In blank dog cytosol matrix, there was no quantifiable human AOX1 peptide signal (Figure 2A), suggesting specificity of the surrogate peptide and absence of interferences from the matrix (AOX deficiency in dogs). The LC-MS/MS method showed robust peptide retention time (7.02 ± 0.02 min) and consistent co-elution of light peptide and stable-isotope labeled internal standard. The dynamic range of current method covered a 3.5-order of magnitude. Furthermore, the narrow CI value ($\pm 5.17\%$) of internal standard peak intensity across the analysis suggested robust analytical performance of this peptide quantitation method. Two other AOX1 surrogate peptides also gave similar linearity, although the LOQ was higher for these two peptides. Among the 20 liver cytosol samples investigated, male cytosols displayed a broader spread of AOX1 levels from 0.74 to 2.30 pmol/mg compared to female cytosols ranging from 0.74 to 1.69 pmol/mg. However, there was no significant gender difference (p-value 0.26) in terms of the averaged AOX1 levels in each gender (Figure 3). The AOX1 concentration in the pooled cytosol lot was 1.71 pmol/mg, which is close to the average (1.41 pmol/mg) of the individual lots. AOX1 levels in the liver cytosols of 8 individual donors were also measured by an orthogonal ELISA method in parallel. Quantitation results using these two different methods correlated well to each other in general as shown in Figure 4. The correlation between the two orthogonal quantitative methods provides confidence on the LC-MS/MS-based AOX1 quantitation method in complex bio-matrices.

***In vitro* AOX1 Activity Measurement and Correlation to the AOX1 Expression Levels**

Intrinsic clearance of the 20 different lots of human cytosol were calculated using Eq. 1 and were summarized in Table 2. For all cytosol samples, carbazeran and phthalazine were depleted much faster than zoniporide, with the average $t_{1/2}$ values of 5.1, 3.7 and 42 min, respectively. The relative activity ranking of the 20 different cytosol samples were consistent among the three substrates (Fig. 5). The half-lives of phthalazine (Fig. 5A) and zoniporide (Fig. 5B) were plotted against those of carbazeran, respectively.. Because of this high concordance of three substrates in reflecting the AOX1 activities,

DMD #53082

clearances of carbazeran were used to represent the AOX1 activities of different cytosol lots and plotted together with the corresponding AOX1 expression levels measured by LC-MS/MS assay (Figure 6). The intrinsic clearance of carbazeran spanned over 90-fold (23 to 2075 $\mu\text{l}/\text{min}/\text{mg}$) among the 20 individual cytosol lots, with 13/20 lots located within the 30% intervals of the median clearance value ($CL_{int, in vitro} \sim 455 \mu\text{l}/\text{min}/\text{mg}$). The AOX1 activity of the pooled lot also acquired a value ($CL_{int, in vitro} \sim 451 \mu\text{l}/\text{min}/\text{mg}$) close to the median value, which is similar to the observation in the AOX1 expression level measurements. Three cytosol lots (F04, M01 and M03) exhibited substantially lower AOX1 activities (below 51 $\mu\text{l}/\text{min}/\text{mg}$ compared to a median value of 455 $\mu\text{l}/\text{min}/\text{mg}$), albeit retained normal AOX1 expression levels. On the other hand, cytosols (M02, M04, and M05) showed abnormally high AOX1 activities (730, 973, and 2075 $\mu\text{l}/\text{min}/\text{mg}$, respectively) and only gave a 20% increase of AOX1 expression level from median value.

Discussion

Individual and Gender Differences in AOX1 Expression and Activity

Individual variation of drug metabolizing enzymes has been observed in terms of expression level and activity, especially for polymorphic enzymes. For example, up to 6.9 fold differences were observed for UGT1A1 expression level in HLM from 16 donors (Sato et al., 2012). In another HLM study (Kawakami et al., 2011), over 20-fold increase of expression levels were observed for several major CYP enzymes (1A2, 2A6, 2C19, and 3A4) in HLM from 10 donors. Individual variability of enzyme activity tended to be greater than that of protein expression level. In a study of AO activities in liver cytosol of eight different strains of rats, substantial difference was observed (as high as 104 folds between Sea/SD strain and WKA/Sea strain) (Kitamura et al., 1999). This is consistent with rats having very variable AO. For activity of human AOX1, over 50 fold spreads were observed using probe substrate, benzaldehyde (Sugihara et al., 1997).

DMD #53082

In this study, up to 3.4 fold difference of AOX1 expression level in cytosol samples were observed from 20 different donors by LC-MS/MS assay. Much greater variations were observed for AOX1 activity based on intrinsic clearance values: 19, 43, and 90 folds were observed when phthalazine, zoniporide, and carbazeran were used as probe substrates, indicating the different sensitivity of probe substrates in AOX1 (Watanabe et al., 1992). The data suggested that the individual differences are minor in AOX1 expression.

Gender differences have been reported for human xenobiotic-metabolizing enzymes such as cytochrome P450s (Hunt et al., 1992; Lamba et al., 2003; Franconi et al., 2007), sulfotransferases (Kocarek et al., 2008), glutathione transferases (Knight et al., 2007), and UDP-glucuronosyltransferases (Ameen et al., 2004; Buckley and Klaassen, 2007). One study with limited sample size (total 6) reported that female mice attained higher AO activity than male mice using selected AO substrates (Watanabe et al., 1992). However, such gender difference vanished when a different substrate was used in the same study. AO activity was compared between male and female mammals using hepatic cytosol system, and noticeable gender difference was observed for mouse (13 fold higher AO activity of male vs. female) but not for other species including human and rat (Klecker et al., 2006). Another study had focused on the human hepatic AOX1 activity and interestingly no difference in AOX1 activity was observed between 10 females and 3 males subjects (Al-Salmy, 2001). In the present study, the sample size was increased to a total of 20 liver cytosols (ten males and ten females donors), and the data showed no significant gender difference (p value= 0.26) in AOX1 expression level by LC-MS/MS (Fig. 3). In terms of activity, male appears to have higher activity than female [average carbazeran intrinsic clearance at 394 (female) and 593 (male) $\mu\text{l}/\text{min}/\text{mg}$, respectively], however the gender difference is not statistically significant for AOX1 activity (p -value = 0.32). There were individuals from both genders (F04, M01 and M03) that

DMD #53082

showed abnormally low AOX1 activities while those with abnormally high AOX1 activities (M02, M04, and M05) are all from the male group (Fig. 6).

Correlation between AOX1 Protein Concentration and Enzyme Activity

For 16 out of the 20 different human liver cytosols in this study, the AOX1 protein levels were distributed in a narrow range between 0.97 and 1.77 pmol/mg (median value: 1.45 pmol/mg and 75% percentile: 1.69 pmol/mg) suggesting relatively low variability in individual protein expression. However, the spread of AOX1 activity was substantial for certain lots despite similar protein expression level. For example, lot M05 had much higher enzyme activity (reason unknown), while lot F04, M01 and M03 exhibited substantially lower AOX1 activities. These results suggest alternative mechanism to manifest AOX1 activity other than AOX1 expression level alone. Possible hypothesis could be a portion of AOX1 were present in various inactive forms (e.g. SNP (Hartmann et al., 2012), Mo cofactor deficiency (Schwarz et al., 2009) and homodimer dissociation (Itoh et al., 2007)), which cannot be identified by the three surrogate peptides in the current LC-MS/MS assay. An additional experiment was conducted to test if the deficiency of molybdenum cofactor could play a role in AOX1 activity. AOX1-bound molybdenum content in lot F04 and the pooled lot (Mix01) were analyzed by ICP-MS, and indeed the Mo concentration in cytosol F04 was 20% lower than that from pooled lot (data not shown). Mo-cofactor needs to be correctly inserted in order for AOX1 to be active (Garattini et al., 2008). The ICP-MS data suggested that active sites of AOX1 in F04 samples may not be fully incorporated with the Mo-cofactor, which would be consistent with the decreased AOX1 activity as compared to normal AOX1. However, this still cannot fully account for the drastic differences of AOX1 activities between these two lots as observed in the carbazeran substrate depletion assay. Other possibilities may also contribute to the low AOX1 activity including protein misfolding, SNP (Hartmann et al., 2012), or chemical/enzymatic modification and disruption of AOX1 homodimer.

DMD #53082

Correlations between Alcohol Usage and AOX1 Activity

The demographic details of the liver cytosol donors revealed that abnormally low AOX1 activities (intrinsic clearance rates for carbazepan at 32 and 23 $\mu\text{l}/\text{min}/\text{mg}$) were observed in two donors with heavy chronic alcohol consumption (M01: 12 pack daily, and F04: 3-4 glass of wine/day for 30yrs). To our best knowledge, this is the first time to observe that heavy chronic alcohol consumption may also lead to significant decrease in AOX1 activity. Interestingly there was no apparent change in enzyme expression level as measured by LC-MS/MS. Other demographic factors, such as age, race, weight, cigarette usage, drug usage, and medication history were not detected to have an impact on AOX1 activity based on this study, albeit the number of samples is too low to make clear conclusions.

Conclusions

In this report, a fast, sensitive, and robust LC-MS/MS method was developed and applied to quantify AOX1 levels in human liver cytosols. The methodology can also be applied for AOX1 quantification in other tissues to aid the development of scaling factor for prediction of *in vivo* clearance of AOX1 substrates and to better understand interindividual variability. The LC-MS measured AOX1 concentrations were in good agreement with those measured by an orthogonal ELISA assay. A relatively narrow spread of AOX1 levels was observed in 20 individual donors (<3.5 fold). *In vitro* AOX1 activities were determined using three representative probe substrates with different sensitivities to human AOX1. Majority of the twenty individual lots showed similar AOX1 activities except for some abnormal lots, where the measured activities could be up to 450% (max value) or 5% (minimal value) of the average. Several lots had very low activity yet retained normal AOX1 protein expression. This suggests It appears that factors other than protein concentration may also affect AOX1 activity; these factors may include protein misfolding, SNP, chemical/enzymatic modification, disruption of AOX1 homodimer, and Mo cofactor deficiency. Further investigation on these areas would help to deepen the understanding of

DMD #53082

the protein expression and activity relationship. Pooling of liver cytosols from multiple donors greatly minimized the impact of individual variability, resulting in a mixture with AOX1 level and activity matched to the averaged values. Our results also suggested that heavy chronic alcohol consumption may lead to marked impairment of AOX1 activity but not the AOX1 expression levels.

DMD #53082

Acknowledgments

We thank Tom McDonald for the discussion around AOX1 protein quantification, Tim Strelevitz for providing the substrate for AOX1 activity assay, and Zhaohui Lei for the help in the ICP-MS experiments.

Authorship Contributions

Participated in research design: Fu, Di, Troutman, Obach, Zhang

Conducted experiments: Fu, Han, Soderstrom, Snyder, Zhang

Performed data analysis: Fu, Di, Zhang

Wrote or contributed to the writing of the manuscript: Fu, Di, Soderstrom, Obach, Zhang

DMD #53082

References:

- Al-Salmi HS (2001) Individual variation in hepatic aldehyde oxidase activity. *IUBMB life* **51**:249-253.
- Ameen C, Linden D, Larsson BM, Mode A, Holmang A, and Oscarsson J (2004) Effects of gender and GH secretory pattern on sterol regulatory element-binding protein-1c and its target genes in rat liver. *American journal of physiology Endocrinology and metabolism* **287**:E1039-1048.
- Anderson L and Hunter CL (2006) Quantitative mass spectrometric multiple reaction monitoring assays for major plasma proteins. *Mol Cell Proteomics* **5**:573-588.
- Buckley DB and Klaassen CD (2007) Tissue- and gender-specific mRNA expression of UDP-glucuronosyltransferases (UGTs) in mice. *Drug Metab Dispos* **35**:121-127.
- Carr SA and Anderson L (2008) Protein quantitation through targeted mass spectrometry: the way out of biomarker purgatory? *Clinical chemistry* **54**:1749-1752.
- Dalvie D, Zhang C, Chen W, Smolarek T, Obach RS, and Loi CM (2010) Cross-species comparison of the metabolism and excretion of zonisamide: contribution of aldehyde oxidase to interspecies differences. *Drug Metab Dispos* **38**:641-654.
- Diamond S, Boer J, Maduskuie TP, Jr., Falahatpisheh N, Li Y, and Yeleswaram S (2010) Species-specific metabolism of SGX523 by aldehyde oxidase and the toxicological implications. *Drug Metab Dispos* **38**:1277-1285.
- Fernandez Ocana M, James IT, Kabir M, Grace C, Yuan G, Martin SW, and Neubert H (2012) Clinical pharmacokinetic assessment of an anti-MAdCAM monoclonal antibody therapeutic by LC-MS/MS. *Analytical chemistry* **84**:5959-5967.
- Franconi F, Brunelleschi S, Steardo L, and Cuomo V (2007) Gender differences in drug responses. *Pharmacological research : the official journal of the Italian Pharmacological Society* **55**:81-95.
- Garattini E, Fratelli M, and Terao M (2008) Mammalian aldehyde oxidases: genetics, evolution and biochemistry. *Cellular and molecular life sciences : CMLS* **65**:1019-1048.
- Garattini E and Terao M (2011) Increasing recognition of the importance of aldehyde oxidase in drug development and discovery. *Drug Metab Rev* **43**:374-386.
- Hartmann T, Terao M, Garattini E, Teutloff C, Alfaro JF, Jones JP, and Leimkuhler S (2012) The impact of single nucleotide polymorphisms on human aldehyde oxidase. *Drug Metab Dispos* **40**:856-864.
- Heikkinen AT, Friedlein A, Lamerz J, Jakob P, Cutler P, Fowler S, Williamson T, Tolando R, Lave T, and Parrott N (2012) Mass spectrometry-based quantification of CYP enzymes to establish in vitro/in vivo scaling factors for intestinal and hepatic metabolism in beagle dog. *Pharm Res* **29**:1832-1842.
- Hunt CM, Westerkam WR, and Stave GM (1992) Effect of age and gender on the activity of human hepatic CYP3A. *Biochem Pharmacol* **44**:275-283.
- Itoh K, Maruyama H, Adachi M, Hoshino K, Watanabe N, and Tanaka Y (2007) Lack of dimer formation ability in rat strains with low aldehyde oxidase activity. *Xenobiotica* **37**:709-716.
- Kawakami H, Ohtsuki S, Kamiie J, Suzuki T, Abe T, and Terasaki T (2011) Simultaneous absolute quantification of 11 cytochrome P450 isoforms in human liver microsomes by liquid chromatography tandem mass spectrometry with in silico target peptide selection. *Journal of pharmaceutical sciences* **100**:341-352.
- Kitamura S, Nakatani K, Sugihara K, and Ohta S (1999) Strain differences of the ability to hydroxylate methotrexate in rats. *Comparative biochemistry and physiology Part C, Pharmacology, toxicology & endocrinology* **122**:331-336.
- Klecker RW, Cysyk RL, and Collins JM (2006) Zebularine metabolism by aldehyde oxidase in hepatic cytosol from humans, monkeys, dogs, rats, and mice: influence of sex and inhibitors. *Bioorganic & medicinal chemistry* **14**:62-66.

DMD #53082

- Knight TR, Choudhuri S, and Klaassen CD (2007) Constitutive mRNA expression of various glutathione S-transferase isoforms in different tissues of mice. *Toxicological sciences : an official journal of the Society of Toxicology* **100**:513-524.
- Kocarek TA, Duanmu Z, Fang HL, and Runge-Morris M (2008) Age- and sex-dependent expression of multiple murine hepatic hydroxysteroid sulfotransferase (SULT2A) genes. *Biochem Pharmacol* **76**:1036-1046.
- Lamba V, Lamba J, Yasuda K, Strom S, Davila J, Hancock ML, Fackenthal JD, Rogan PK, Ring B, Wrighton SA, and Schuetz EG (2003) Hepatic CYP2B6 expression: gender and ethnic differences and relationship to CYP2B6 genotype and CAR (constitutive androstane receptor) expression. *The Journal of pharmacology and experimental therapeutics* **307**:906-922.
- Li H, Kundu TK, and Zweier JL (2009) Characterization of the magnitude and mechanism of aldehyde oxidase-mediated nitric oxide production from nitrite. *The Journal of biological chemistry* **284**:33850-33858.
- Li N, Nemirovskiy OV, Zhang Y, Yuan H, Mo J, Ji C, Zhang B, Brayman TG, Lepsy C, Heath TG, and Lai Y (2008) Absolute quantification of multidrug resistance-associated protein 2 (MRP2/ABCC2) using liquid chromatography tandem mass spectrometry. *Anal Biochem* **380**:211-222.
- Moriwaki Y, Yamamoto T, Takahashi S, Tsutsumi Z, and Hada T (2001) Widespread cellular distribution of aldehyde oxidase in human tissues found by immunohistochemistry staining. *Histol Histopathol* **16**:745-753.
- Neumeier M, Weigert J, Schaffler A, Weiss TS, Schmidl C, Buttner R, Bollheimer C, Aslanidis C, Scholmerich J, and Buechler C (2006) Aldehyde oxidase 1 is highly abundant in hepatic steatosis and is downregulated by adiponectin and fenofibric acid in hepatocytes in vitro. *Biochem Biophys Res Commun* **350**:731-735.
- Pryde DC, Dalvie D, Hu Q, Jones P, Obach RS, and Tran TD (2010) Aldehyde oxidase: an enzyme of emerging importance in drug discovery. *J Med Chem* **53**:8441-8460.
- Rashidi MR, Smith JA, Clarke SE, and Beedham C (1997) In vitro oxidation of famciclovir and 6-deoxypenciclovir by aldehyde oxidase from human, guinea pig, rabbit, and rat liver. *Drug Metab Dispos* **25**:805-813.
- Sakamoto A, Matsumaru T, Ishiguro N, Schaefer O, Ohtsuki S, Inoue T, Kawakami H, and Terasaki T (2011) Reliability and robustness of simultaneous absolute quantification of drug transporters, cytochrome P450 enzymes, and Udp-glucuronosyltransferases in human liver tissue by multiplexed MRM/selected reaction monitoring mode tandem mass spectrometry with nano-liquid chromatography. *Journal of pharmaceutical sciences* **100**:4037-4043.
- Sato Y, Nagata M, Kawamura A, Miyashita A, and Usui T (2012) Protein quantification of UDP-glucuronosyltransferases 1A1 and 2B7 in human liver microsomes by LC-MS/MS and correlation with glucuronidation activities. *Xenobiotica* **42**:823-829.
- Schwarz G, Mendel RR, and Ribbe MW (2009) Molybdenum cofactors, enzymes and pathways. *Nature* **460**:839-847.
- Seibert C, Davidson BR, Fuller BJ, Patterson LH, Griffiths WJ, and Wang Y (2009) Multiple-approaches to the identification and quantification of cytochromes P450 in human liver tissue by mass spectrometry. *J Proteome Res* **8**:1672-1681.
- Sugihara K, Kitamura S, Tatsumi K, Asahara T, and Dohi K (1997) Differences in aldehyde oxidase activity in cytosolic preparations of human and monkey liver. *Biochemistry and molecular biology international* **41**:1153-1160.
- Watanabe K, Matsunaga T, Narimatsu S, Yamamoto I, and Yoshimura H (1992) Sex difference in hepatic microsomal aldehyde oxygenase activity in different strains of mice. *Research communications in chemical pathology and pharmacology* **78**:373-376.

DMD #53082

Weigert J, Neumeier M, Bauer S, Mages W, Schnitzbauer AA, Obed A, Groschl B, Hartmann A, Schaffler A, Aslanidis C, Scholmerich J, and Buechler C (2008) Small-interference RNA-mediated knock-down of aldehyde oxidase 1 in 3T3-L1 cells impairs adipogenesis and adiponectin release. *FEBS Lett* **582**:2965-2972.

Williamson BL, Purkayastha S, Hunter CL, Nuwaysir L, Hill J, and Easterwood L (2011) Quantitative protein determination for CYP induction via LC-MS/MS. *Proteomics* **11**:33-41.

DMD #53082

Figure Legends

Figure 1: LC-MS/MS quantitation method development for AOX1 surrogate peptides on 5600 Triple TOF and LTQ Velos platforms. Upper panel shows the selected MRM transitions for the three AOX1 surrogate peptides ($^{446}\text{VFFGEGDGIIR}^{456}$, $^{779}\text{YIQDIVASTLK}^{789}$ and $^{813}\text{TGIIAAVTAFANK}^{826}$) digested from recombinant AOX1 protein. The signal intensity of the peptides is in the order of VFF > YIQ > TGI. For the liver cytosol samples, the same set of AOX1 surrogate peptides were monitored by MRM^{HR} mode. Significant matrix ion suppression was observed, leading to substantial reduction of MRM signals for the peptides of interest. In the bottom panel, the preliminary MRM^{HR} method was transferred to a refined pseudo-MRM method performed on a LTQ-Velos instrument with extended chromatographic time of 15 min. Signal-to-noise ratio (S/N) was enhanced by almost 3-fold for all three peptides with 5 times more diluted samples compared to the liver cytosol sample used in the MRM^{HR} mode.

Figure 2: Calibration curve of AOX1 peptide VFFGEGDGIIR prepared in digested dog liver cytosol. The blank matrix (digested dog liver cytosol) did not show traceable interference to the peptide of interest. The LC-MS method showed robust peptide retention time (7.02 ± 0.02 min) and co-elution of light peptide and stable isotope-labeled internal standard (SIS, upper-right corner). Standard curve covered the concentration range of VFF peptide from 6.25 pg/ml to 25 ng/ml with excellent linearity (Bottom right corner, $Y=1.4230X - 0.1313$, $R^2=0.9994$). The insert of calibration plot showed excellent linearity in the low concentration range (6.25 pg/ml to 1.25 ng/ml).

Figure 3: Distribution of AOX1 protein levels in 20 liver cytosols with individual donors. AOX1 levels were measured by AQUA LC-MS/MS methods (as described in the method section). A narrow range of AOX1 concentration distribution was observed between 0.74 and 2.30 pmol/mg. There is no significant gender differences between the two groups (p value = 0.26). However, female samples exhibit slightly tighter AOX1 concentration distribution (0.74 to 1.69 pmol/mg) compared to those of the male samples (0.74 to 2.30 pmol/mg).

DMD #53082

Figure 4: Correlation of AOX1 quantitation results by two orthogonal methods (ELISA and LC-MS/MS) using liver cytosol samples from 8 donors. Linear relationship between these two quantitation methods was attained with the exclusion of two outliers (M4 and M5). For the 6 liver cytosols used for the fitting, ELISA method gave lower AOX1 expression values compared to the LC-MS/MS method. This may reflect the differences (antigen-antibody binding affinity, purity, and dimer formation) between recombinant AOX1 standard proteins and endogenous AOX1 protein in the corresponding matrices.

Figure 5: Comparison of *in vitro* AOX1 activity (expressed as substrate half-lives) of different cytosol lots using different substrates: strong correlations can be observed between half lives of phthalazine and those of carbazeran (A), as well as between half lives of zoniporide and those of carbazeran (B).

Figure 6: Correlation between *in vitro* AOX1 activity ($CL_{int, in vitro}$, $\mu\text{l}/\text{min}/\text{mg}$) measured by substrate depletion of carbazeran and AOX1 concentration (pmol/mg) determined by LC-MS/MS method. The plot is arranged in the order of increasing AOX1 activities from left to right for the 20 individual cytosol and the pooled lot.

DMD #53082

Table 1. MRM Conditions for the Three AOX1 Substrates.

Analyte	Q1	Q3	DP (v)	CE (v)
Carbazeran	360.9	272.1	80	30
Zoniporide	321.2	262.2	60	30
Phthalazine	131.1	104.0	60	30

DP: Declustering Potential; CE: Collision Energy.

DMD #53082

Table 2. Intrinsic Clearance of the Three AOX1 Substrates in 21 Human Liver Cytosols.

Lot ID	$CL_{int, in vitro}$ ($\mu\text{l}/\text{min}/\text{mg}$)		
	Carbazeran	Zoniporide	Phthalazine
F01	485±25	32.6±0.6	592±64
F02	132±7	9.6±0.7	363±59
F03	544±40	49.0±1.5	624±25
F04	23±2	3.6±0.4	36±9
F05	464±33	34.4±3.0	525±39
F06	500±52	42.2±2.8	586±90
F07	457±40	31.9±2.3	609±67
F08	448±120	34.2±2.6	631±77
F09	467±102	44.2±1.4	587±77
F10	423±58	30.2±0.9	500±54
M01	32±22	11.0±15.6	36±4
M02	730±144	153.6±4.2	352±115
M03	51±1	5.7±0.3	126±8
M04	973±21	73.1±1.8	336±14
M05	2075±125	147.5±4.0	620±51
M06	453±85	35.0±6.1	604±62
M07	304±4	21.3±3.1	623±8
M08	502±58	50.2±4.1	537±26
M09	435±67	35.1±1.0	603±29
M10	379±6	20.5±0.6	578±51
Pooled lot	451±39	30.0±1.7	612±91

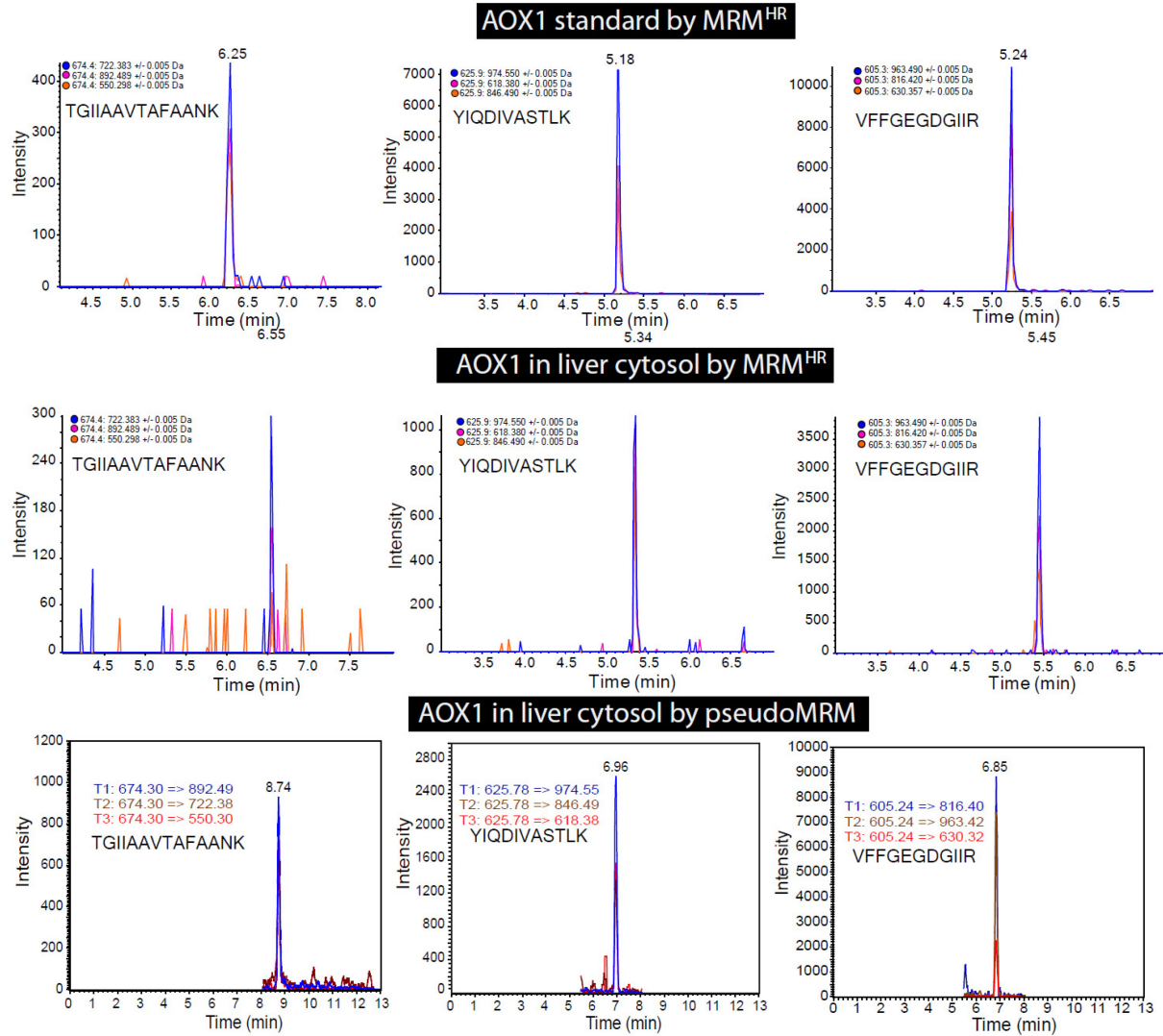


Figure 1.

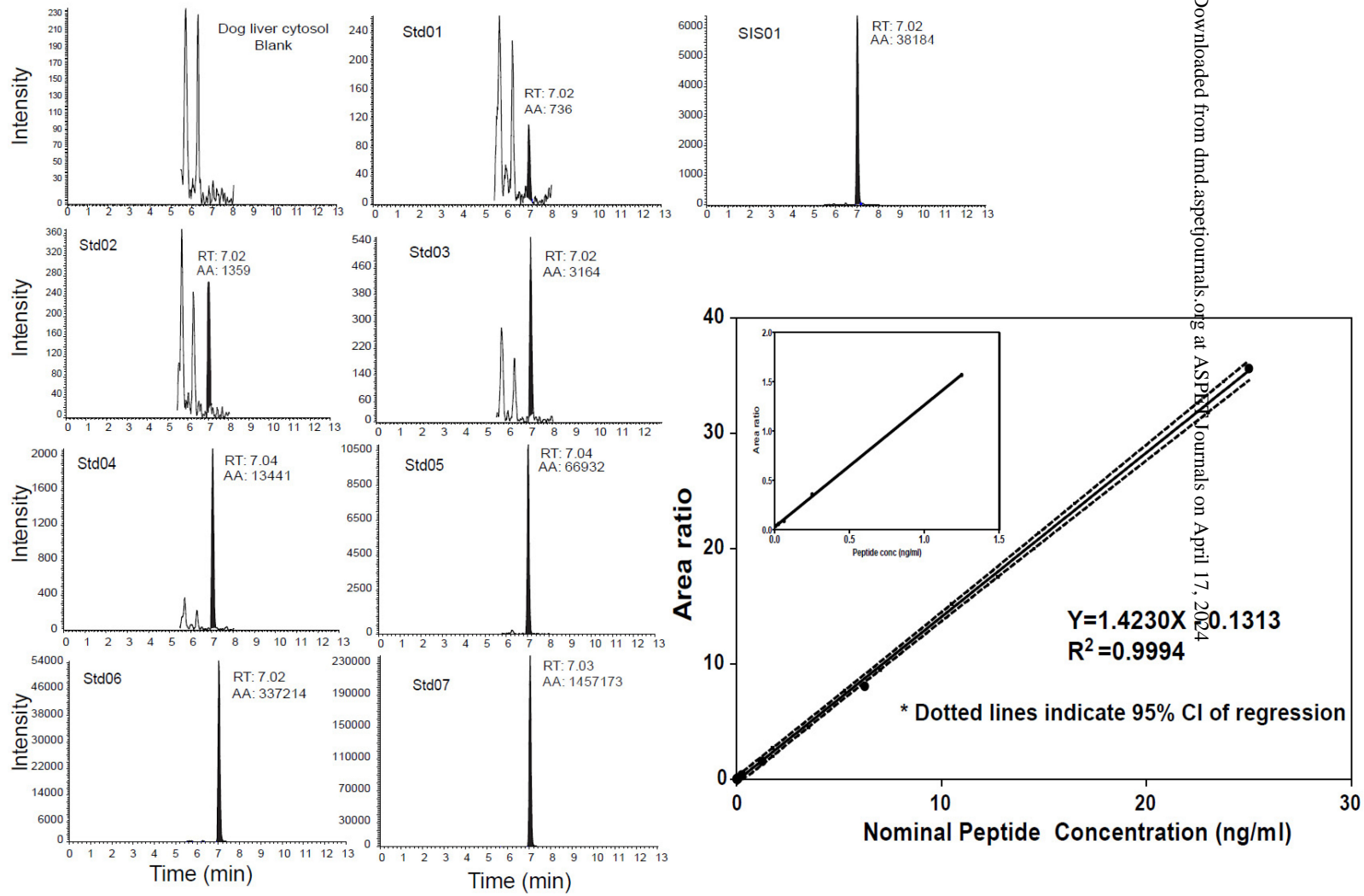


Figure 2.

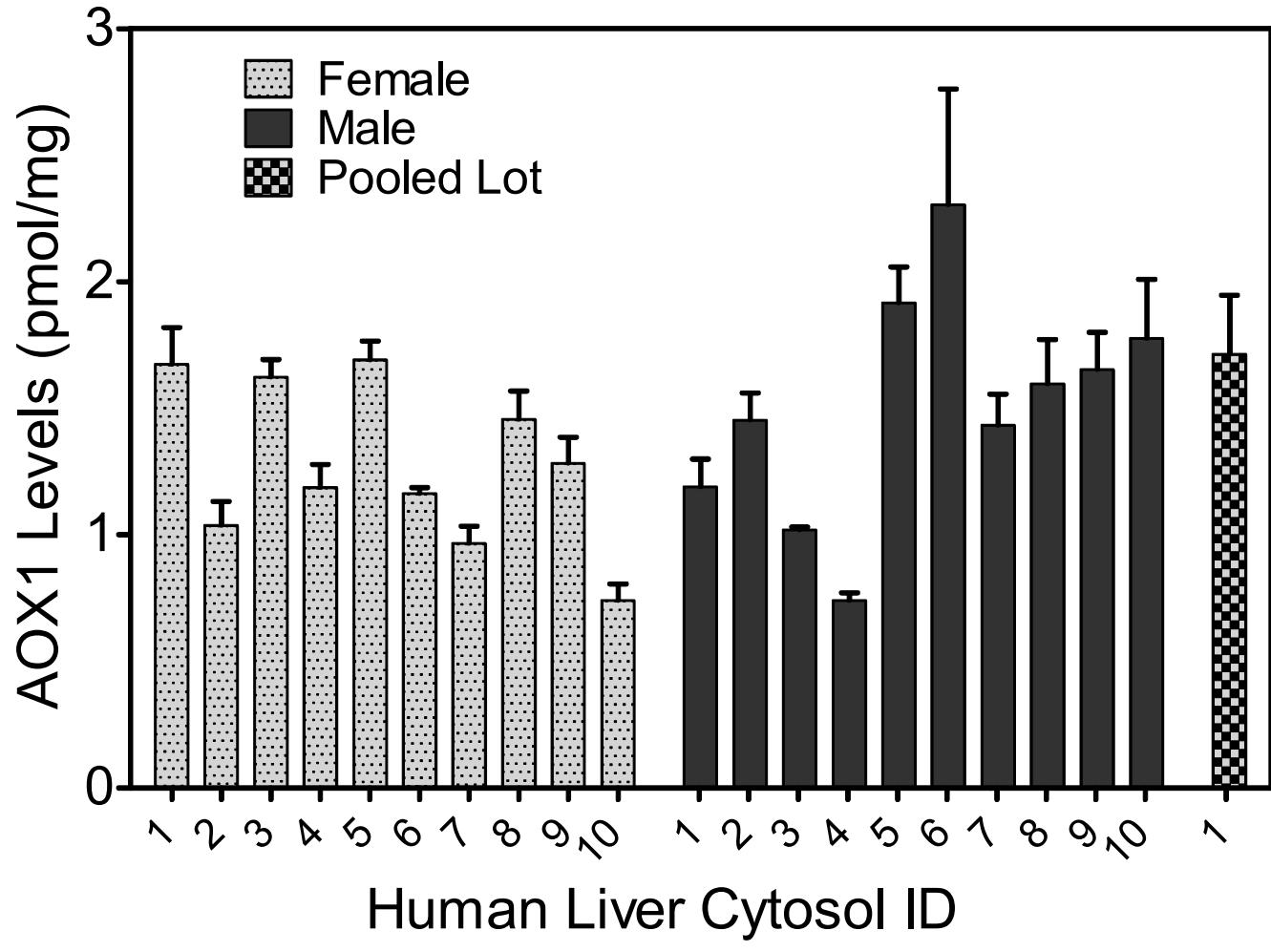


Figure 3.

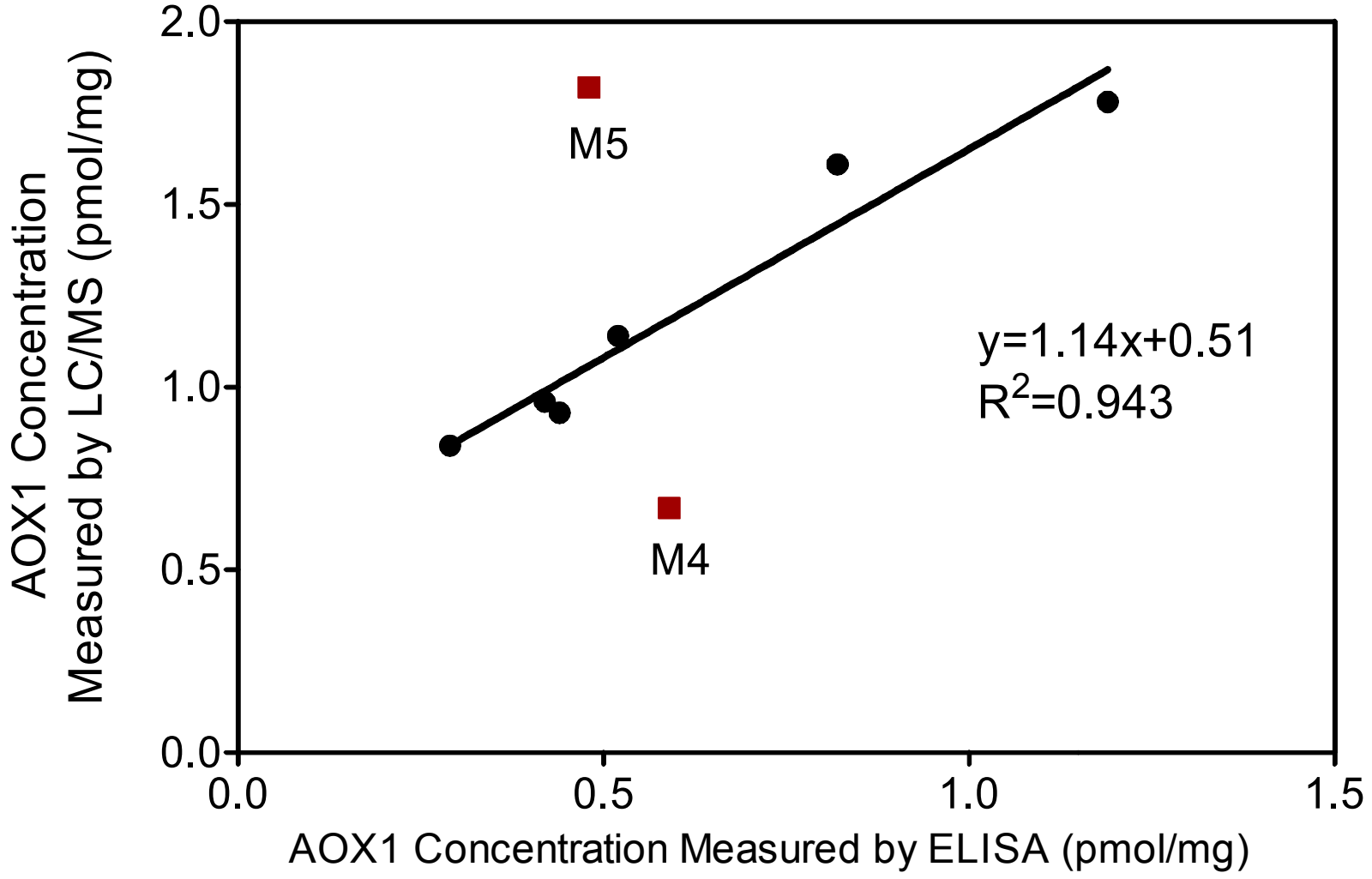


Figure 4.

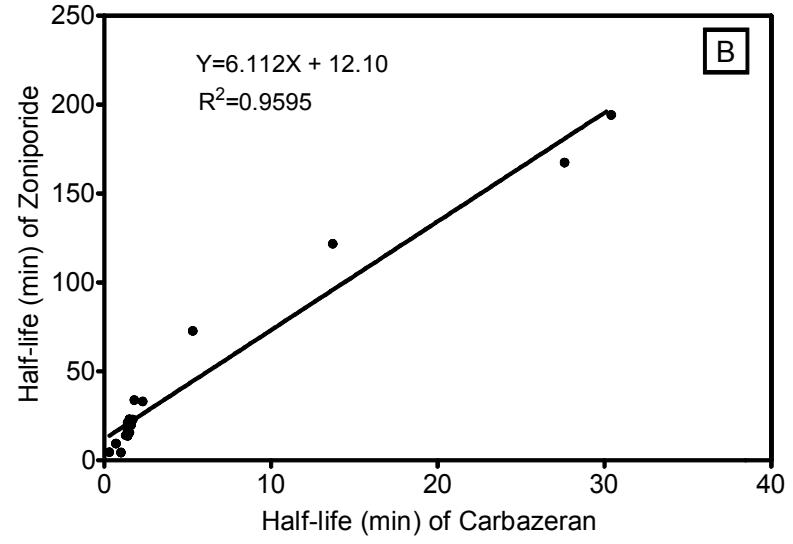
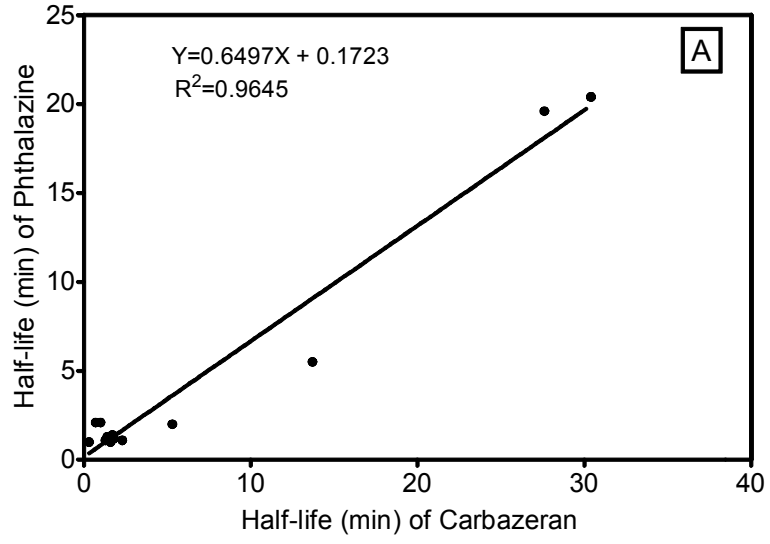


Figure 5.

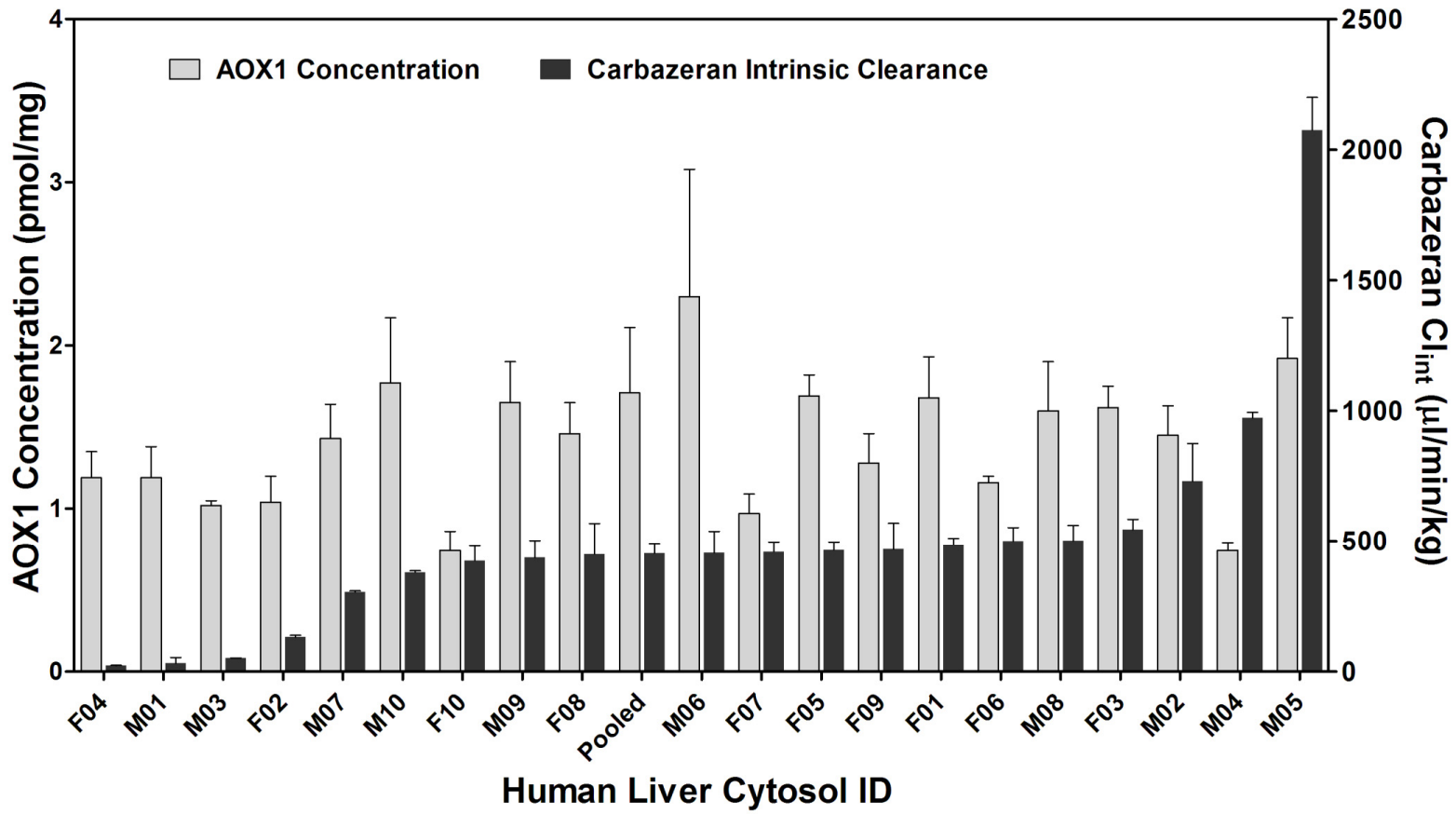


Figure 6.